Journal of Solid State Chemistry **161,** 396–401 (2001)
doi:10.1006/jssc.2001.9354, available online at http://www.idealibrary.com on IDEAL®

Structure of Al Defect in High-Temperature Superconductor, Al-Doped Sm-123: An Electron Density Study

Marco Scavini*,[1] and Riccardo Bianchi†

*Dipartimento di Chimica Fisica ed Elettrochimica, Università di Milano, via C. Golgi, 19, I-20133 Milano, Italy; and †Centro di Studio per le relazioni tra Sruttura e Reattività chimica, CNR, via C. Golgi, 19, I-20133 Milano, Italy

Received May 2, 2001; in revised form July 30, 2001; accepted August 9, 2001

Two Sm-123 single crystals of composition $Sm_{1.06}Ba_{1.94}Cu_{2.65}Al_{0.35}O_{6+\delta}$ ($0 \leq \delta \leq 1$) were annealed under reducing ($T = 750°C$, $P(O_2) = 10^{-4}$ atm) and oxidizing ($T = 400°C$, $P(O_2) = 10^{-1}$ atm) conditions. Their investigations by X-ray diffraction at room temperature evidence that both reduced and oxidized samples belong to the same space group, *P4/mmm*. Aluminum substitutes copper only at the (0, 0, 0) crystallographic position and it displaces to the ($\cong 0.06$, $\cong 0.06$, 0) site. Two oxygen ions in the basal plane are bonded to each Al ion. Both (0, $\frac{1}{2}$, 0) and ($\frac{1}{2}$, 0, 0) sites are occupied by oxygen ions so that Al ions are in a tetrahedral coordination. The local structural distortion, induced by aluminum substitution, inhibits the tetragonal → orthorhombic phase transition. © 2001 Academic Press

Key Words: **high T_C superconductors; point defects; crystal structure and symmetry; X-ray diffraction.**

1. INTRODUCTION

The cation substitutions in $RBa_2Cu_3O_{6+\delta}$ ($R =$ Y, Ln; $0 \leq \delta \leq 1$) high T_c superconductors (R-123) were widely studied in order to understand their physical properties in the normal and the superconducting states (1–12). In most cases efforts were focused on copper substitutions, because chains and planes of Cu and O ions are involved in the mechanism of superconductivity.

Most of the papers mentioned have investigated Y-123 (1–11) while a few works have considered the case of Ln-123 (1, 6, 12). In Y-123 compounds, some cations like Zn (2–4) and Ni (2–5) substitute the Cu2 (0, 0, $\cong$0.35) site, while Al (2, 5–7, 12) and Co (8) ions enter in the Cu1 (0, 0, 0) site. Finally, there is evidence that Li (9) and Fe (10) substitute copper in the two mentioned positions, depending on the doping level and on the annealing route. However, for an exhaustive discussion on this subject, see (1) and references therein.

The magnetic nature of the dopant seems to be less important than the substitution site for the superconducting properties (5); generally, doping in the Cu2 site lowers T_c more than doping in the Cu1 site (8).

The aim of this paper is to determinate the Al defect structure by means of X-ray diffraction (XRD) and of nuclear magnetic resonance in Al-doped Sm-123 superconductor.

This work is part of a wider study dealing with the effect of Al substitution on the physical properties of Sm-123 superconductor. The choice of aluminum as a substituent is due to the Al^{3+} ion closed-shell electron configuration; this feature should make easier the calculation of carrier concentration in the Cu2 and O superconducting planes.

In order to understand the effect of Al substitution in Sm-123 on its physical properties it is essential to determine the structural model of the doped compound, i.e., the effect of doping around Al dopant (short-range structure) and its consequence on the long-range structure.

2. EXPERIMENTAL DETAILS

Single crystals of $Sm_{1.06}Ba_{1.94}Cu_{2.65}Al_{0.35}O_{6+\delta}$ were prepared by Dr. Maurizio Ferretti at the University of Genova (13, 14).

Electron micro probe analysis (EMPA) inspection was performed with a Jeol JXA840A equipped with three wavelength-dispersive X-ray spectrometers, on a fragment of a single crystal. Data collection was carried out at 20 kV and 20 nA. For each element a calibration was carried out by means of natural/synthetic standards. In particular for aluminum a natural Kaersutite standard was used. The cationic composition, obtained by averaging 10 measurements, is Sm : Ba : Cu : Al = 1.06(3) : 1.94(4) : 2.65(5) : 0.35(2).

Polycrystalline samples were synthesized by solid state reaction of BaO_2 (Aldrich, 95%), Sm_2O_3, CuO, and Al_2O_3 (all Aldrich, 99.99%); the starting mixture stechiometry was chosen on the basis of the EMPA results.

Powders were mixed, pressed into pellets, and allowed to react in pure oxygen at 960°C for a total time of 72 h with one intermediate cooling, grinding, and repelletization.

---

[1] To whom correspondence should be addressed. Fax + 39-02-70638129. E-mail: marco.scavini@unimi.it.

0022-4596/01 $35.00

The as-prepared mono- and polycrystalline Sm-123 samples were annealed in quartz ampoules either under reducing or oxidizing conditions. The annealing routes were 360 h at $T = 750°\mathrm{C}$ and $P(\mathrm{O}_2) = 10^{-4}$ atm, followed by quenching to room temperature for the "reduced samples," and 360 h at $T = 400°\mathrm{C}$ and $P(\mathrm{O}_2) = 10^{-1}$ atm with subsequent quenching to room temperature for the "oxidized samples."

Thermogravimetric analysis on polycrystalline samples revealed that $\delta = 0.80$ for the oxidized and $\delta = 0.40$ for the reduced samples (15).

For single-crystal X-ray analysis two disk-shaped samples of $0.07 \times 0.07 \times 0.03\ \mathrm{mm}^3$ (reduced) and $0.08 \times 0.08 \times 0.04\ \mathrm{mm}^3$ (oxidized) were mounted on a Syntex P4 four-circle diffractometer, using graphite-monochromatized Mo$K\alpha$ ($\lambda = 0.71073$ Å) radiation. Intensity data were collected at 293 K up to $2\theta = 113°$ with ω–2θ scan method and they were corrected for Lorenz, polarization, and absorption effects. Table 1 summarizes the experimental details.

Structure solution (direct methods) and preliminary structure refinements were performed with use of the SHELX97 program (16). The final refinements of scale factor, extinction, positional, temperature, and occupation parameters were carried on with the VALRAY program implemented by Stewart and Spackman (17). Sm^{3+}, Ba^{2+}, Cu^{2+}, Al^{3+}, and O^{-} scattering factors and anomalous scattering factors were taken from *International Tables for Crystallography* (18).

^{27}Al MAS-NMR data were collected with an AMX400WB spectrometer (Bruker, Germany, $B_0 = 9.4$ T) at Larmor frequency of 104.2 MHz. The spectra were acquired using a 4-mm probehead (Bruker) equipped with cylindrical zirconia rotors and a boron nitride stator. The samples were spun at 13.5 kHz with a 15° pulse of 0.4 μs and a recycle time of 1 s. The small flip angle was chosen in order to allow a semiquantitative estimate of the ^{27}Al ($I = \frac{5}{2}$) central transition (19). As usual, in order to calibrate the energy scale, the ^{27}Al chemical shift is referenced to $\mathrm{Al(H_2O)_6^{3+}}$ (20).

TABLE 1
Crystal Data for Reduced (Red.) and Oxidized (Ox.) Samples

Formula	Red.	$\mathrm{Sm_{1.06}Ba_{1.94}Cu_{2.65}Al_{0.35}O_{6.40}}$
	Ox.	$\mathrm{Sm_{1.06}Ba_{1.94}Cu_{2.65}Al_{0.35}O_{6.80}}$
Formula weight	Red.	706.08
	Ox.	712.48
Space group		*P*4/*mmm*
Z value		1
μ (Mo$K\alpha$)		$26.80\ \mathrm{mm}^{-1}$
Temperature		293 K
Radiation		0.71073 (Mo$K\alpha$)
Scan type		ω–2θ
Scan rate		1°/min
Scan width		$1.0° + \Delta\theta_{\alpha_1,\alpha_2}$
2θ range	Red.	$3.5 \leq 2\theta \leq 113.0°$
	Ox.	$3.5 \leq 2\theta \leq 113.3°$
Sphere of data		$\pm h, \pm k, +l$
No. of independent	Red.	769
reflections	Ox.	776
Cell parameter *a* (Å)	Red.	3.9012(2)
	Ox.	3.9067(2)
Cell parameter *c* (Å)	Red.	11.7679(6)
	Ox.	11.7375(9)

3. RESULTS AND DISCUSSION

Pure $\mathrm{SmBa_2Cu_3O_{6+\delta}}(\delta \cong 0)$ crystallizes in the *P*4/*mmm* tetragonal space group (21). With the addition of oxygen it undergoes a tetragonal → orthorhombic phase transition and, when $\delta \cong 1$, the space group is *Pmmm* (21).

As shown in Table 1, both reduced and oxidized Al-doped Sm-123 samples belong to the *P*4/*mmm* tetragonal space group, as previously found for Al-doped Y-123 (2, 5).

Figure 1 shows a schematic drawing of a Sm-123 unit cell. In the asymmetric unit are present Sm1 at $(\frac{1}{2}, \frac{1}{2}, \frac{1}{2})$, Ba at $(\frac{1}{2}, \frac{1}{2}, z)$, Cu1 at (0, 0, 0), Cu2 at $(0, 0, z)$, O1 at $(0, 0, z)$, O2 at $(0, \frac{1}{2}, z)$ and O3 at $(0, \frac{1}{2}, 0)$ sites.

Sm1, Ba,[2] Cu2, O1, and O2 sites were found fully occupied from X-ray analysis; in contrast, Cu1 and O3 special positions revealed a lack of electron density with respect to the full occupation.

Preliminary X-ray refinement for the reduced sample led to an estimate of 0.38 ions per cell for O3 occupation factor ($\delta = 0.38$), in good agreement with thermogravimetric findings ($\delta = 0.40$) (15). It is important to note that pure Sm-123, annealed under similar experimental conditions, shows lower oxygen content ($\delta = 0.18$) (22).

Analogous agreement was found for the oxidized sample between X-ray refinement ($\delta = 0.82$) and thermogravimetric results ($\delta = 0.80$) (15).

For both samples, the cationic occupations from EMPA revealed, in comparison to the Sm:Ba:Cu 1:2:3 stoichiometric formula, a deficiency of Cu that is balanced by Al giving the cationic ratio, Sm:Ba:Cu:Al 1.06:1.94:2.65:0.35. From X-ray data analysis, we observed that the Cu2 site is full occupied, so we can infer that, as in Al-doped Y-123 compound (5), all Al ions revealed by EMPA are located at the Cu1 electron-deficient site, where the Cu/Al atomic ratio is approximately 0.65/0.35.

In order to estimate the actual position of Al ions additional full-matrix refinements were performed for both samples setting 0.65 for Cu1 and zero for Al occupation factors.

The Fourier difference density (FDD) maps are shown in Fig. 2. The maps are through the planes parallel to the *c* axis and passing to Cu1 ions for the reduced (Fig. 2a) and oxidized (Fig. 2b) samples.

---

[2] We will not discuss the small Sm substitution on the Ba site (Sm2), as it is not important for the following discussion.

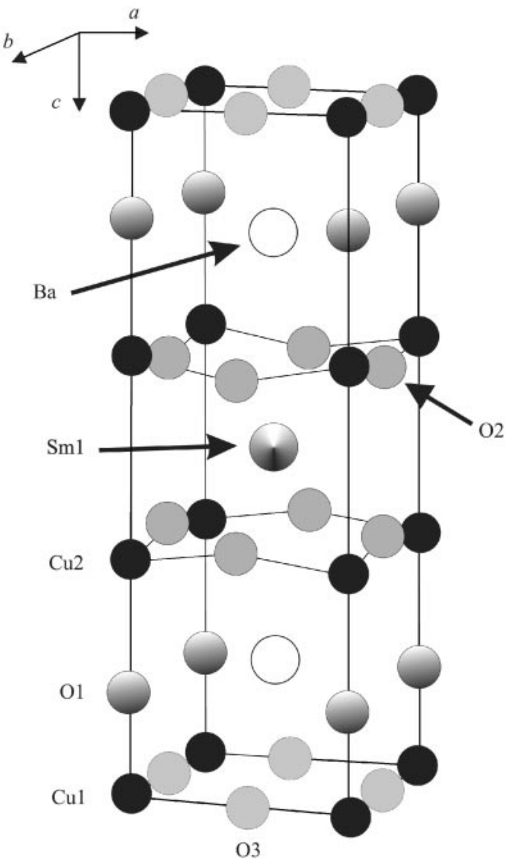

FIG. 1. Schematic drawing of Sm-123. The space group is *P*4/*mmm*. Cu1 and O3 sites are partially occupied.

In Fig. 2a around each Cu1 site four residual peaks (max. about 7 e/Å^3) are evident in ($\pm x, \pm x, 0$) symmetry-equivalent positions with fractional coordinate $x = 0.059$. It is interesting to note that the residual density steeply decreases approaching the (0, 0, 0) special position. A similar trend is shown in Fig. 2b ($x = 0.063$); for both samples no significant density residuals around the Cu2 sites (not shown) are present.

The high peaks close to Cu1 ions of the two samples (Figs. 2a and 2b) cannot be ascribed to a nonbonding charge density; in fact the FDD on the same planes calculated by Buttner *et al.* (23) on a Y-123 pure sample does not show significant residuals around Cu1 ions. This suggests that they should be associated with disordered aluminum, which was not considered in the previous refinements.

In the final structural model, Al ion was positioned at the ($x, x, 0$) special position for reduced ($x = 0.059$) and oxidized ($x = 0.063$) samples. In order to avoid strong correlation among Al and Cu1 parameters, the aluminum and the other ion parameters were alternatively refined. Only the last four cycles were carried out through full-matrix refinement. The final results for reduced and oxidized samples are shown in Table 2.

Fixing the occupation factor of Al at the EMPA value of 0.35 atoms per formula, the electronic populations of 12.1(6) and 13(1) electrons per atom (see Table 2) were determined from the least-squares procedure for reduced and oxidized samples, respectively.

In Fig. 3 are shown the final FDD maps for the two samples on the planes parallel to the *c* axis containing Cu1 and Al ions. No significant density peaks around Cu1 sites are present anymore. We can reasonably infer that the high peaks present in the FDD maps of Figs. 2a and 2b are associated with Al dopant ions slightly shifted with respect to the Cu1 sites. So, the final structural model gives a quantitative interpretation of disorder due to copper substitution by aluminum in the crystal structure. To our knowledge this is the first time that the actual Al dopant position in high-temperature superconductors was experimentally determined.

In order to gain more information about the local structure of aluminum, ^{27}Al NMR measurements were performed on both reduced and oxidized polycrystalline samples.

The two curves of Fig. 4 have a high peak at 74 ppm which is associated with the tetrahedral environment of Al ions (7, 20). A less apparent peak can be noted at 14 ppm for both samples, indicating that few nuclei (1–2%) are involved in an octahedral site symmetry. NMR results clearly indicate that almost all Al ions are in a tetrahedral coordination, independent of the annealing conditions.

On the basis of X-ray diffraction and NMR results the following model for Al defect structure in Sm-123 can be suggested.

Aluminum substitutes copper on the Cu1 site (35% of site substitution in our samples) and at the same time it displaces to ($x, x, 0$), with $x \cong 0.06$. In space group *P*4/*mmm* four equivalent ($\pm x, \pm x, 0$) sites are present; when an Al ion substitute copper only one of the four equivalent sites is occupied, and the space group symmetry is statistically saved. The ($x, x, 0$) site occupation, expressed as atoms per site in our samples, is ≈ 0.09.

Around each Al only two of the four O3 sites in ($\frac{1}{2}, 0, 0$) and ($0, \frac{1}{2}, 0$) special positions are occupied by oxygen ions, determining, together with the two O1 ions at ($0, 0, z$) and ($0, 0, -z$) positions, a tetrahedral environment. As a matter of fact, the resulting Al–O distances indicate a distorted tetrahedral coordination: d(Al–O3) = 1.74(2) Å, in accordance with the Al–O distance reported by Shannon and Prewitt for a tetrahedral coordination (24), while d(Al–O1) = 1.82(1) is a bit longer.

It is reasonable to suppose that around Al, in agreement with NMR results, oxygen O1 ions are slightly displaced with respect to their crystallographic position (see Table 2), in order to reduce the distortion.

An indirect confirmation of the last hypothesis could be inferred from the analysis of the thermal ellipsoids (see

TABLE 2

Atomic Fractional Coordinates, Anisotropic Temperature (Å^2), Site Occupation Factors (Atoms per Cell), and Electron Populations (Electrons per Atom) for the Reduced (Red.) and Oxidized (Ox.) Samples[a]

Atom		x/a	y/b	z/c	U_{11}	U_{22}	U_{33}	Site occupation	Electron population
Sm1	Red.	0.5	0.5	0.5	0.00676(9)	$\equiv U_{11}$	0.0116(1)	1	59.9(2)
	Ox.				0.00688(9)		0.0084(1)		59.4(3)
Sm2		≡ Ba	≡ Ba	≡ Ba	≡ Ba	≡ Ba	≡ Ba	0.06	≡ Sm1
Ba	Red.	0.5	0.5	0.19103(3)	0.0135(1)	$\equiv U_{11}$	0.0139(1)	1.94	54.5(2)
	Ox.			0.18805(3)	0.0143(1)		0.0113(1)		54.6(2)
Cu1	Red.	0	0	0	0.0160(6)	$\equiv U_{11}$	0.0112(8)	0.65	≡ Cu2
	Ox.				0.0160(5)		0.0064(5)		
Cu2	Red.	0	0	0.35550(7)	0.0059(1)	$\equiv U_{11}$	0.0156(3)	2	27.7(2)
	Ox.			0.35470(6)	0.0067(1)		0.0126(3)		27.9(2)
Al	Red.	0.059(4)	$\equiv x$	0	0.017(6)	$\equiv U_{11}$	0.029(9)	0.35	12.1(6)
	Ox.	0.063(4)			0.026(9)		0.053(13)		13(1)
O1	Red.	0	0	0.1518(5)	0.030(2)	$\equiv U_{11}$	0.018(2)	2	≡ O2
	Ox.			0.1542(6)	0.033(3)		0.019(3)		
O2	Red.	0.5	0	0.3733(3)	0.0051(8)	0.0077(9)	0.015(1)	4	9.4(1)
	Ox.			0.3734(3)	0.0057(8)	0.0086(9)	0.0122(9)		9.3(1)
O3	Red.	0	0.5	0	0.034(16)	0.011(9)	0.015(9)	0.40	≡ O2
	Ox.				0.030(8)	0.015(5)	0.016(5)	0.80	
$R(F) = \sum \lVert F_o\rvert - k\lvert F_c \rVert / \sum \lvert F_o \rvert =$	Red.			0.0353	$wR(F) = [\sum w(\lvert F_o\rvert - k\lvert F_c\rvert)^2 / \sum w \lvert F_o \rvert^2]^{1/2}$			Red.	0.0330
	Ox.			0.0382				Ox.	0.0382

[a] The anisotropic temperature factor is defined by $\exp\{-8\pi^2[(ha^*/2)^2 U_{11} + (kb^*/2)^2 U_{22} + (lc^*/2)^2 U_{33}]\}$. F_o and F_c are the observed and calculated structure factors, $w = 1/\sigma^2(F_o)$ and k is the scale factor.

Table 2). In fact the U_{11} and U_{22} components of O1 atoms are about 4–6 times higher with respect to the corresponding ones of O2 atoms, suggesting that they could include both thermal and static (distortion) disorder.

Figures 2–4 and Table 2 show that the XRD and NMR results for reduced and oxidized samples are close, apart from O3 site occupation factor. In particular, both Al displacement (see Figs. 2, 3 and Table 2) and aluminum envi-

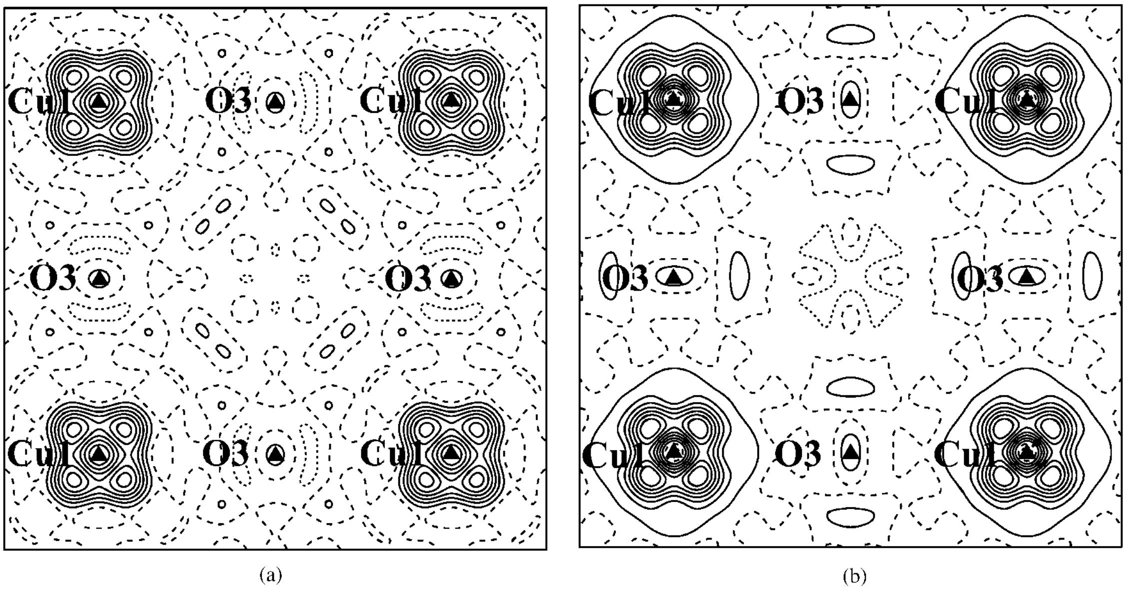

(a)

(b)

FIG. 2. Fourier difference density maps on the (001) planes, obtained without aluminum in the structural model. The maps (a) and (b) are through the Cu1 ions for the reduced and oxidized samples, respectively. Triangles evidence ion positions. Contour intervals at 1 e/Å^3. Solid lines represent positive contour, short dashed lines represent negative contour, and wide dashed line represents zero contour.

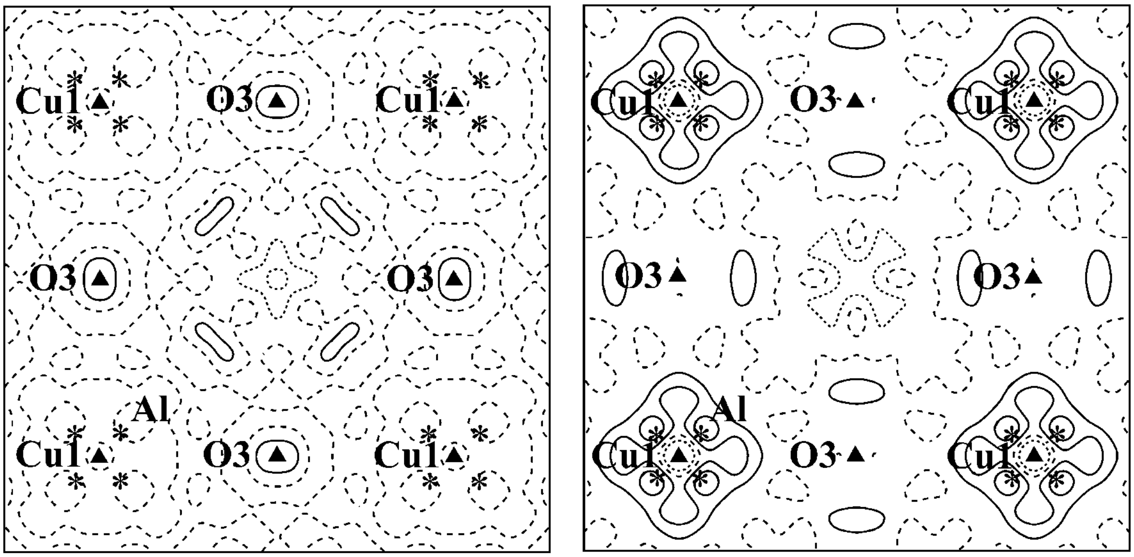

(a) (b)

FIG. 3. As the corresponding Figs. 2a and 2b, but calculated from a structural model which includes aluminum. Triangles evidence Cu and O ion positions. Asterisks evidence the disordered aluminum positions.

ronment (see Fig. 4) are quite similar. Moreover, thermogravimetric analysis has revealed that for reduced Al-doped Sm-123 the O3 occupation factor is 0.40 atoms per formula unit (15), while for pure Sm-123 it is 0.18 atoms per formula unit (22). All these experimental findings indicate that, in the reduced sample, the oxygen ions in O3 sites are pinned to Al ions, as proposed for Al-doped Y-123 superconductor (5). When oxygen is introduced in the structure by annealing under oxidizing conditions, the extra oxygen is positioned at O3 sites near Cu ions, so that the Al environment does not vary.

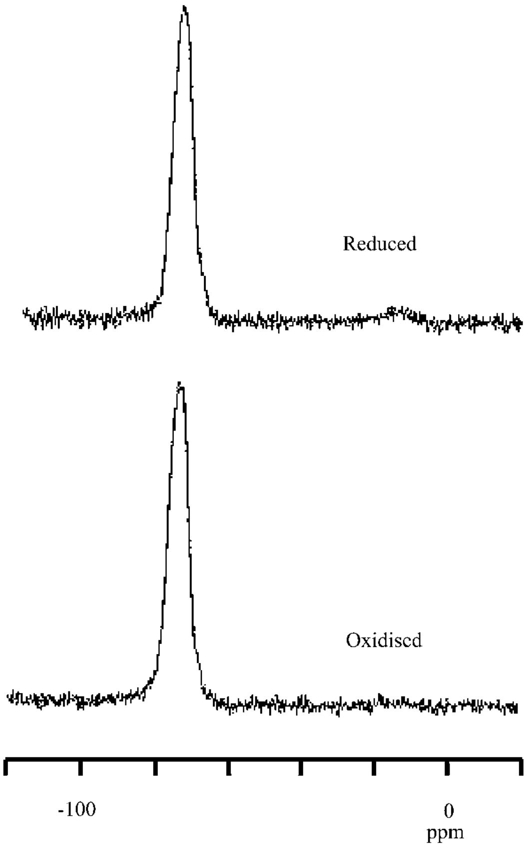

FIG. 4. ^{27}Al MAS-NMR spectra of aluminum-doped Sm-123 for reduced and oxidized polycrystalline samples.

The local structural rearrangement around Al ions influences also the long-range structure. In fact, the simultaneous occupation by O3 ions of the ($\frac{1}{2}$, 0, 0) and (0, $\frac{1}{2}$, 0) sites among the aluminium ions statistically saves the symmetry of the tetragonal *P*4/*mmm* space group also in the oxidized sample. In contrast, in undoped samples, when oxygen enters in the structure by annealing under oxidizing conditions, O3 ions order along the *b* direction, determining a tetragonal → orthorhombic phase transition (21).

ACKNOWLEDGMENTS

The authors gratefully thank Dr. Piercarlo Mustarelli who performed the NMR measurements, Dr. Maria Pia Riccardi who performed SEM-EMPA determinations, and Dr. Maurizio Ferretti who produced the single crystals.

REFERENCES

1. M. S. Skakle, *Mater. Sci. Eng.* **R23,** 1 (1998) and references therein.
2. T. Takabatake and M. Ishikawa, *Solid State Commun.* **66,** 413 (1988).
3. R. P. Gupta and M. Gupta, *Phys. Rev. B* **59,** 3381 (1999).
4. M. A. Rodriguez, A. Navrotsky, and F. Licci, *Physica C* **329,** 88 (2000).
5. E. Brecht, W. W. Schmahl, G. Miehe, M. Rodewald, H. Fuess, N. H. Andersen, J. Hanssmann, and Th. Wolf, *Physica C* **265,** 53 (1996).

6. T. Siegrist, L. F. Schneemeyer, J. V. Waszczak, N. P. Singh, R. L. Opila, B. Batlogg, L. W. Rupp, and D. W. Murphy, *Phys. Rev. B* **36,** 8365 (1987).
7. R. Dupree, A. Gencten, and D. McK. Paul, *Physica C* **193,** 81 (1992).
8. J. M. Tarascon, P. Barboux, P. F. Miceli, L. H. Greene, G. W. Hull, M. Eibschutz, and S. A. Sunshine, *Phys. Rev. B* **37,** 7458 (1988).
9. F. Maury, M. Nicolas-Francillon, F. Bourée, R. Ollitrault-Fichet, and M. Nanot, *Physica C* **333,** 121 (2000).
10. S. K. Nikogosyan, A. A. Sahakyan, H. N. Yeritsyan, V. A. Grigoryan, E. G. Zargaryan and A. G. Sarkissyan, *Physica C* **299,** 65 (1998).
11. M. S. Islam and C. Ananthamohan, *Phys. Rev. B* **44,** 9492 (1991).
12. S. Uma, G. Rangarajan, and E. Gmelin, *Physica C* **301,** 141 (1998).
13. M. Ferretti, E. Magnone, and G. L. Olcese, *Physica C* **235–240,** 311 (1994).
14. E. Magnone, M. Ferretti, and G. L. Olcese, *Il Nuovo Cimento* **16D,** 1679 (1994).
15. Malavasi *et al.* Work in progress.
16. G. M. Sheldrick, "SHELX-97: A program for structure refinement." Univ. of Gottingen, Gottingen, Germany, 1997.
17. R. F. Stewart and M. A. Spackman, "Valray User's Manual." Department of Chemistry, Carnegie-Mellon University, Pittsburgh, PA, 1983.
18. J. A. Ibers and W. C. Hamilton, "International Tables for X-ray Crystallography," Vol. IV, Chap. 2.2. Kynoch Press, Birmingham, 1974.
19. S. M. Bradley and J. V. Hanna, *J. Am. Chem. Soc.* **116,** 7771 (1994).
20. G. Engelhardt and D. Michel, "High Resolution Solid-state NMR of Silicates and Zeolites." Wiley, Chichester, 1987.
21. M. Guillaume, P. Allenspach, W. Henggeler, J. Mesot, B. Roessli, U. Staub, P. Fischer, A. Furrer, and V. Trounov, *J. Phys.*: *Condens. Matter* **6,** 7963 (1994)
22. G. Chiodelli, I. Wenneker, P. Ghigna, G. Spinolo, G. Flor, M. Ferretti, and E. Magnone, *Physica C* **308,** 257 (1998)
23. R. H. Buttner, E. N. Maslen, and N. Spadaccini, *Acta Crystallogr. B* **48,** 21 (1992).
24. R. D. Shannon and C. T. Prewitt, *Acta Crystallogr. B* **25,** 925 (1969).